



Synthesis of bitetrathiafulvalenes with FeCl₃-mediated homo-coupling of tetrathiafulvalenylmagnesium bromide and formation of nanostructures from bitetrathiafulvalenes having long alkylthio chains

Yohei Honna^a, Eigo Isomura^a, Hideo Enozawa^a, Masashi Hasegawa^b, Masayoshi Takase^a, Tohru Nishinaga^a, Masahiko Iyoda^{a,*}

^a Department of Chemistry, Graduate School of Science and Engineering, Tokyo Metropolitan University, Hachioji, Tokyo 192-0397, Japan

^b Department of Chemistry, School of Science, Kitasato University, Sagami-hara, Kanagawa 228-8555, Japan

ARTICLE INFO

Article history:

Received 8 October 2009

Revised 19 November 2009

Accepted 24 November 2009

Available online 27 November 2009

ABSTRACT

The FeCl₃-mediated homo-coupling of 4,5-bis(alkylthio)-4'-tetrathiafulvalenylmagnesium bromide **5** produced the corresponding bitetrathiafulvalene derivatives **2a–d** in moderate yields (25–51%). Bitetrathiafulvalenes **2c** and **2d** having long alkylthio chains formed nanostructures and showed bulk electric conductivities ($\sigma_{\text{rt}} = 2.6 - 8.0 \times 10^{-5} \text{ S cm}^{-1}$) in the neutral state owing to the fastener effect. Interestingly, the nanofiber of tetrakis(dodecylthio)bitetrathiafulvalene **2d** exhibited a p-type semiconductivity as detected by AFM.

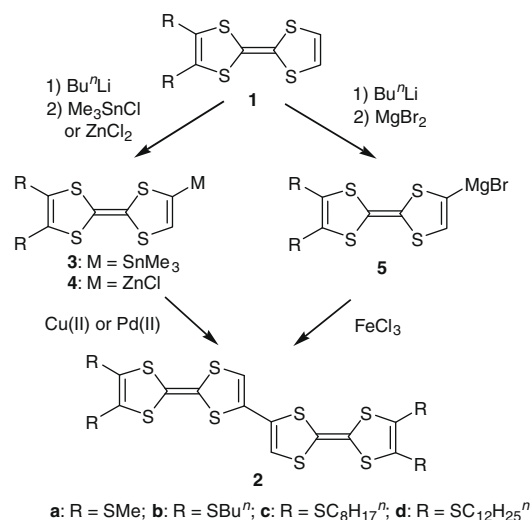
© 2009 Elsevier Ltd. All rights reserved.

During the course of our studies of tetrathiafulvalene (TTF) oligomers,¹ we needed bitetrathiafulvalenes **2** (bi-TTFs) with long alkylthio side chains.² The stacking ability of TTFs increases with the lengthening of alkylthio chains, known as the fastener effect,³ because the van der Waals interactions between alkyl chains fasten the central TTF-moieties tightly in the direction for enhancing molecular overlap.⁴ Therefore, bi-TTFs **2** with long alkylthio chains can be expected to show better molecular overlap and better electric conductivities in the neutral and cation radical states, together with nanostructure formation owing to their amphiphilic properties.⁵ Although the synthesis of bi-TTFs **2** by the homo-couplings of organotin⁶ and organozinc intermediates **3** and **4** has been reported,^{6,7} we have newly developed a one-pot procedure for the synthesis of bi-TTFs **2** by the homo-coupling of highly reactive organomagnesium intermediates **5** with FeCl₃ (Scheme 1). This method can be applied to the homo-coupling of rather unreactive TTFs having long alkylthio chains. We report here the successful synthesis of bi-TTFs **2c** and **2d** having octylthio and dodecylthio side chains, together with the formation of their nanofibers.

Since TTFs **1** are unstable under acidic condition, all reactions should be conducted under neutral or basic condition. In addition, some coupling reagents easily oxidize the starting material **1** and the product **2**.

Therefore, the reagents for the coupling reaction are restricted to weak oxidants working under mild experimental conditions. Thus, we first reported the coupling of **3** using Pd(II) or Cu(II) re-

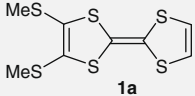
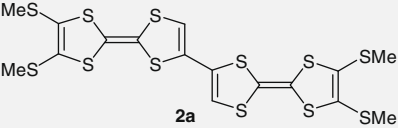
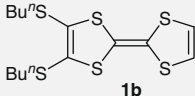
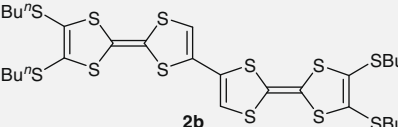
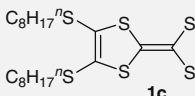
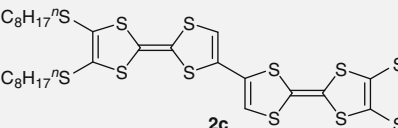
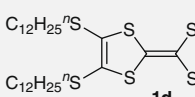
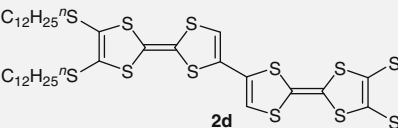
agent.^{6,7a} Since this procedure requires the isolation of **3**, we then developed the coupling of **4** with PdCl₂(PPh₃)₂.^{7c} This reaction produces **2** in moderate yields, but the low reactivity of organozinc intermediate sometimes produces **2** in low yields. Therefore, we attempted the formation of organomagnesium intermediates **5** to produce bi-TTFs **2** by the homo-coupling reaction (Scheme 1, Table 1).



Scheme 1. Synthesis of Bi-TTFs.

* Corresponding author. Tel.: +81 42 677 2547; fax: +81 42 677 2525.
E-mail address: iyoda@tmu.ac.jp (M. Iyoda).

Table 1
Synthesis of bi-TTFs **2a–d** via TTF–MgBr **5a–d** (Scheme 1)^a

Entry	Starting material	Conditions (equivalent)	Product	Yield ^b (%)
1	 1a	(i) Bu ⁿ Li (1.2), (ii) MgBr ₂ (1.6), (iii) FeCl ₃ (1.0), –10 °C, 1 h	 2a	6
2		(i) Bu ⁿ Li (1.2), (ii) MgBr ₂ (1.6), (iii) FeCl ₃ (2.0), –10 °C, 1 h		31
3		(i) Bu ⁿ Li (1.2), (ii) MgBr ₂ (1.6), (iii) FeCl ₃ (3.0), –10 °C, 1 h 25 °C, 1 h		30
4		(i) Bu ⁿ Li (1.2), (ii) MgBr ₂ (1.6); (iii) FeCl ₃ (2.0), –10 °C, 1 h 25 °C, 1 h		51
5	 1b	(i) Bu ⁿ Li (1.2), (ii) MgBr ₂ (1.6); (iii) FeCl ₃ (2.0), –10 °C, 2 h 25 °C, 1 h	 2b	25
6	 1c	(i) Bu ⁿ Li (1.2), (ii) MgBr ₂ (1.6); (iii) FeCl ₃ (2.0), –10 °C, 1 h 25 °C, 1 h	 2c	36
7	 1d	(i) Bu ⁿ Li (1.2), (ii) MgBr ₂ (1.6); (iii) FeCl ₃ (2.0), –10 °C, 1 h 25 °C, 1 h	 2d	43

^a The reaction of **1a–d** with butyllithium (1.2 equiv), followed by treatment with MgBr₂ (1.6 equiv) produced **5a–d**, which were reacted with FeCl₃ (1.0–3.0 equiv) at –10 or 25 °C for 1–2 h.

^b Isolated yield.

The synthesis of bi-TTFs **2a–d** is summarized in Table 1. To optimize the reaction conditions, the coupling reaction of 4,5-bis(methylthio)-TTF **1a** was first examined. The reaction of **1a** with butyllithium (1.2 equiv) was carried out at –78 to –65 °C in THF, followed by treatment with dry MgBr₂ (1.6 equiv) at –65 °C for 1 h and then by warming to –20 °C to afford tetrathiafulvalenyl magnesium bromide **5a**.⁸ At –20 °C, a solution of FeCl₃ (1.0 equiv) in THF was added and the mixture was stirred at –10 °C for 2 h to produce a bi-TTF derivative **2a**^{7c} in 6% yield (entry 1). However, a similar reaction of **5a** with 2.0 and 3.0 equiv of FeCl₃ at –10 °C for 2 h afforded **2a** in 31% and 30% yields, respectively (entries 2 and 3). Thus, 2.0 equiv of FeCl₃ forces the reaction to completion. Furthermore, the reaction of **5a** with FeCl₃ at 25 °C for 1 h afforded **2a** in 51% yield (entry 4). Based on the result obtained from the reaction of **1a**, the reactions of **1b**, **1c**, and **1d** were carried out (entries 5–7). Although the reaction of the oily **1b** gave **2b**⁹ in 25% yield (entry 5), the crystalline **1c** and **1d** produced the corresponding bi-TTFs **2c** and **2d** in 36% and 43% yields, respectively (entries 6 and 7).^{10,11} For the synthesis of **2d**, the treatment of organozinc species **4d** with PdCl₂(PPh₃)₂ (1.0 equiv) or FeCl₃ (2.0 equiv) afforded **2d** in 23% and 11% yields, respectively. Thus, the oxidation of **5d** produces **2d** in higher yields than that of **4d**.

All bi-TTFs **2a–d** are stable crystalline solids and show reversible redox waves, as determined by the measurement of redox potential using cyclic voltammetry (CV).¹² As shown in Table 2, **2a–d** exhibit higher oxidation potentials than **1d**, indicating their lower HOMO levels. The small separation of the first oxidation potentials of **2a–d** reflects a weak through-bond interaction between the two TTF units in **2a–d**.^{1f} The bulk conductivities of **2c** and **2d** shown in Table 2 are higher than those of **2a** and

Table 2
Redox potentials^a and electric conductivities^b of **2a–d**

Compd	$E^{\text{ox}1}_{1/2}$ (V)	$E^{\text{ox}2}_{1/2}$ (V)	σ_{rt} (S cm ⁻¹)
1d	–0.03	0.36	–
2a	0.09 ^d	0.42	7.9×10^{-7e} 1.1×10^{-6f}
2b	0.09 ^d	0.47	3.8×10^{-7e}
2c	0.10 ^d	0.47	2.6×10^{-5e}
2d	0.10 ^d	0.49	8.0×10^{-5e}

^a Conditions: 0.1 M Bu₄NClO₄ in dichloromethane, Ag/Ag⁺ reference electrode, Pt working electrode and Pt counterelectrode, 100 mV s⁻¹.

^b Room-temperature conductivity measured in a pellet by a two-probe technique.

^c V versus Fc/Fc⁺. Fc/Fc⁺ = 0.29 V referred to Ag/Ag⁺.

^d The first oxidation potential shows a small peak separation owing to the formation of the corresponding cation radical and dication. The first potentials of **2a–d** are as follows. **2a**: 0.07 and 0.11 V; **2b**: 0.06 and 0.12 V; **2c**: 0.08 and 0.12 V; **2d**: 0.09 and 0.11 V.

^e Measured using a compressed pellet.

^f Measured using a single crystal.

2b,¹³ although the redox potentials of **2b–d** are almost the same.³ As reported previously,^{7c} the crystal structure of **2a** shows a slipped plane-to-plane stacking with the planarity of the central S₂C₂–C₂S₂ unit, and the face-to-face distance between the almost planar bi-TTF units is 3.61 Å. However, there is no side-by-side interaction between the bi-TTF units, and the conductivity ($\sigma_{\text{rt}} = 1.1 \times 10^{-6}$ S cm⁻¹) of **2a** crystal in Table 2 reflects its crystal structure. Furthermore, the bulk conductivities of **2a** and **2b** ($\sigma_{\text{rt}} = 7.9 \times 10^{-7}$ and 3.8×10^{-7} S cm⁻¹, respectively) are similar probably owing to either weak π – π or S–S interaction. In the case of **2c** and **2d**, their conductivities ($\sigma_{\text{rt}} = 2.6 \times 10^{-5}$ and

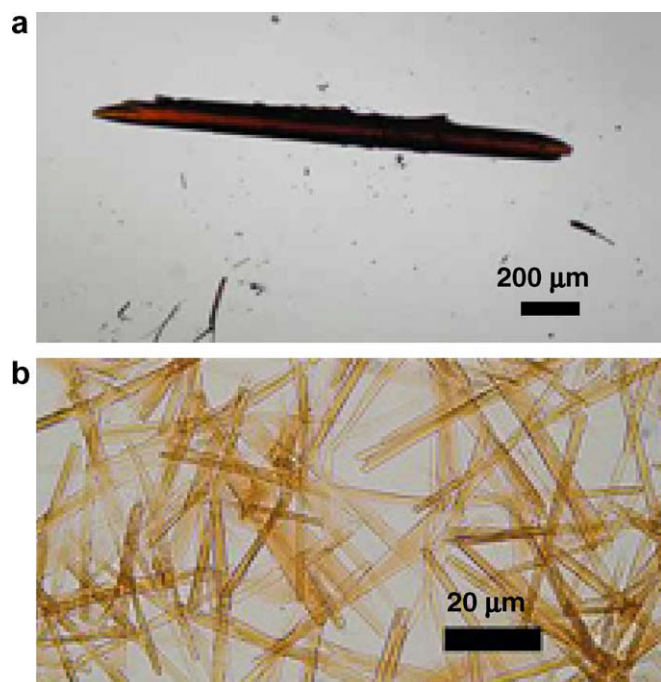


Figure 1. Needle-like morphologies prepared from **2b** (a) and **2d** (b) in CH_2Cl_2 .

$8.0 \times 10^{-5} \text{ S cm}^{-1}$, respectively) increase, because the van der Waals interaction between the long alkyl chains fasten the central bi-TTF moiety (the fastener effect) to induce stronger π – π and S–S interactions.

As has been reported, TTF derivatives with a long alkyl chain self-aggregate into a one-dimensional columnar structure in the solid state.¹⁴ To utilize this effect in the construction of electroactive nanostructures, we examined the formation of nanostructures from **2b–d**. The butylthio and dodecylthio derivatives **2b** and **2d** form needle-like structures from CH_2Cl_2 (Fig. 1a and b). As shown in Figure 2a and b, X-ray diffractometry (XRD) of needle-like morphologies of **2b** and **2d** revealed different internal structures. Thus, the XRD profile of **2b** needles shows a fairly high crystallinity (Fig. 2a). In contrast, **2d** shows a regular reflection pattern (Fig. 2b), and the strong (1 0 0) reflection at $2\theta = 2.21^\circ$ ($d = 40 \text{ \AA}$) can be assigned to the molecular size, whereas weak reflections at $2\theta = 4.42^\circ$ (2 0 0), 6.63° (3 0 0), and 8.84° (4 0 0) are higher-order reflections. Since a weak reflection at $2\theta = 22.2^\circ$ ($d = 4.0 \text{ \AA}$) can be assigned to the (0 0 1) reflection,¹⁵ **2d** needles have a stacked lamellar structure, in which **2d** may be oriented perpendicularly to the long axis of the needle-like fiber. In accord with the stacking structure of the **2d** fiber, the doping of a compressed pellet with iodine vapor produced a black conductive pellet ($\sigma_{\text{rt}} = 1.3 \times 10^{-2} \text{ S cm}^{-1}$). Interestingly, the **2d** fiber on graphite was shown to exhibit p-type semiconducting spectroscopic curves when probed by current sensing AFM.^{16,17} This p-type semiconducting behavior is caused by the fastened lamellar structure of the **2d** fiber.

In summary, the homo-coupling of TTFs **1a–d** having long alkylthio units has been carried out using the iron-mediated oxidative coupling of tetrathiafulvalenylmagnesium bromides **5a–d** in moderate yields. Bi-TTF derivatives **2c** and **2d** showed higher electric conductivities than **2a** and **2b** owing to the fastener effect. Furthermore, the direct conductivity measurement of the **2d** fiber by current-sensing AFM exhibited p-type semiconducting properties on account of a stacked lamellar structure.

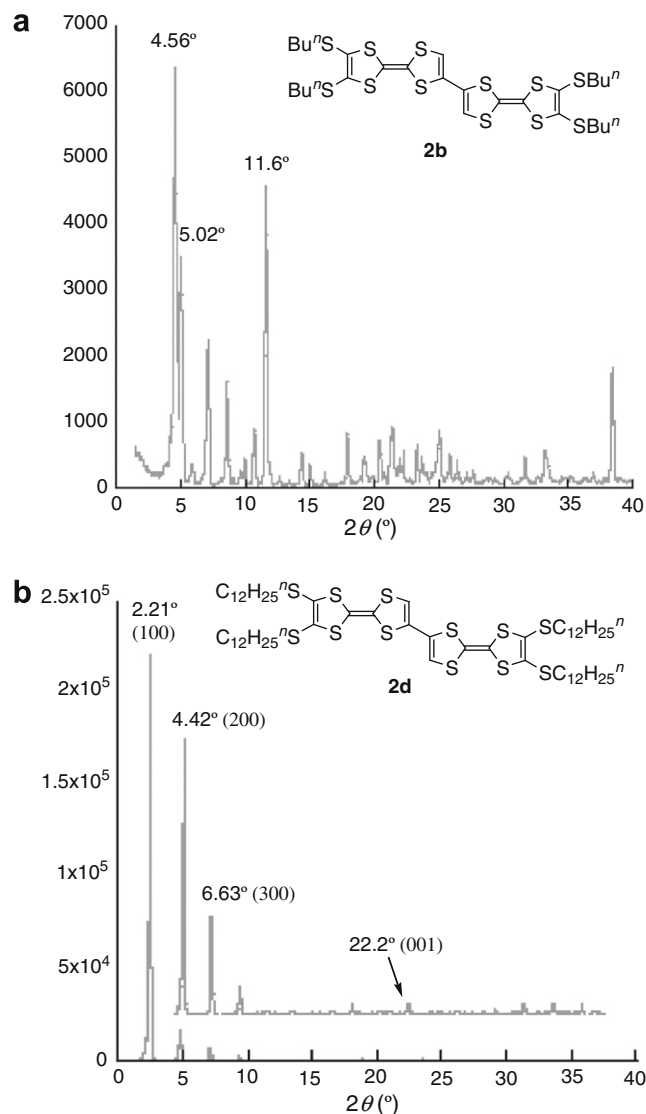


Figure 2. XRD profiles of the **2b** needle (a) and **2d** needle-like nanostructure (b). The inset in Figure 2b shows a ninefold expansion.

Acknowledgments

This work was supported in part by a Grant-in-Aid for scientific research from JSPS. We would like to thank Professor K. Mizoguchi and Professor K. Kikuchi (Tokyo Metropolitan University) for their assistance with the conductivity measurement and Mr. S. Ishimoto and Y. Kobayashi for their experimental assistance. The authors are greatly indebted to Mr. Akinori Kogure and Mr. Yasunobu Kajifusa (Shimadzu Corp.) for their measurement of the semiconducting properties of the **2d** fiber by current sensing AFM.

Supplementary data

Supplementary data associated with this article can be found, in the online version, at doi:10.1016/j.tetlet.2009.11.106.

References and notes

- (a) Iyoda, M.; Hasegawa, M.; Miyake, Y. *Chem. Rev.* **2004**, *104*, 5085–5113; (b) Iyoda, M. Bi- and Bis-TTFs. In *TTF Chemistry*; Yamada, J., Sugimoto, T., Eds.; Springer: Tokyo, 2004; (c) Iyoda, M.; Ogura, E.; Hara, K.; Kuwatani, Y.; Nishikawa, H.; Sato, T.; Kikuchi, K.; Ikemoto, I.; Mori, T. *J. Mater. Chem.* **1999**, *9*,

- 335–337; (d) Iyoda, M.; Sasaki, S.; Miura, M.; Fukuda, M.; Yamauchi, J. *Tetrahedron Lett.* **1999**, *40*, 2807–2810; (e) Iyoda, M.; Hasegawa, M.; Kuwatani, Y.; Nishikawa, H.; Fukami, K.; Nagase, S.; Yamamoto, G. *Chem. Lett.* **2001**, 1146–1147; (f) Iyoda, M.; Hasegawa, M.; Takano, J.; Hara, K.; Kuwatani, Y. *Chem. Lett.* **2002**, 590–591; (g) Hasegawa, M.; Takano, J.; Enozawa, H.; Kuwatani, Y.; Iyoda, M. *Tetrahedron Lett.* **2004**, *45*, 4109–4112; (h) Iyoda, M.; Enozawa, H.; Miyake, Y. *Chem. Lett.* **2004**, 1098–1099; (i) Hara, K.; Hasegawa, M.; Kuwatani, Y.; Enozawa, H.; Iyoda, M. *Chem. Commun.* **2004**, 2042–2043; (j) Hasegawa, M.; Kobayashi, Y.; Hara, K.; Enozawa, H.; Iyoda, M. *Heterocycles* **2009**, *77*, 837–842.
2. For the synthesis of bi-TTFs, see: (a) Kreitsberga, Y. N.; Édzhinya, A. S.; Kampare, R. B.; Neiland, O. Y. *Zh. Org. Khim.* **1989**, *25*, 1456–1462. *J. Org. Chem. USSR*, **1989**, 1312–1317; (b) Tatemitsu, H.; Nishikawa, E.; Sakata, Y.; Misumi, S. *Synth. Met.* **1987**, *19*, 565–568; (c) Lerstrup, K.; Jørgensen, M.; Johannsen, I.; Bechgaard, K. In *The Physics and Chemistry of Organic Superconductors*; Ishiguro, T., Yamaji, K., Saito, G., Eds.; Springer: Berlin, 1990; p 383; (d) Becker, J. Y.; Bernstein, J.; Ellern, A.; Gershtenman, H.; Khodorkovsky, V. *J. Mater. Chem.* **1995**, *5*, 1557–1558; (e) Sako, K.; Kusakabe, M.; Watanabe, T.; Tatemitsu, H. *Synth. Met.* **1995**, *71*, 1949–1950; (f) Sako, K.; Kusakabe, M.; Watanabe, T.; Takamura, H.; Shinmyozu, T.; Tatemitsu, H. *Mol. Cryst. Liq. Cryst.* **1997**, *296*, 31–40; (g) John, D. E.; Moore, A. J.; Bryce, M. R.; Batsanov, A. S.; Howard, J. A. K. *Synthesis* **1998**, 826–828; (h) John, D. E.; Moore, A. J.; Bryce, M. R.; Batsanov, A. S.; Howard, J. K. A. *J. Mater. Chem.* **2000**, *10*, 1273–1279.
3. Inokuchi, H.; Saito, G.; Seki, K.; Wu, P.; Tang, T. B.; Mori, T.; Imaeda, K.; Enoki, T.; Higuchi, Y.; Inaka, K.; Yasuoka, N. *Chem. Lett.* **1986**, 1263–1266.
4. Saito, G.; Yoshida, Y. *Bull. Chem. Soc. Jpn.* **2007**, *80*, 1–137.
5. (a) Enozawa, H.; Hasegawa, M.; Takamatsu, D.; Fukui, K.; Iyoda, M. *Org. Lett.* **2006**, *8*, 1917–1920; (b) Hasegawa, M.; Enozawa, H.; Kawabata, Y.; Iyoda, M. *J. Am. Chem. Soc.* **2007**, *129*, 3072–3073; (c) Kobayashi, Y.; Hasegawa, M.; Enozawa, H.; Iyoda, M. *Chem. Lett.* **2007**, *36*, 720–721; (d) Iyoda, M.; Hasegawa, M.; Enozawa, H. *Chem. Lett.* **2007**, *36*, 1402–1407; (e) Enozawa, H.; Honna, Y.; Iyoda, M. *Chem. Lett.* **2007**, *36*, 1434–1435; (f) Hasegawa, M.; Enozawa, H.; Iyoda, M. *J. Synth. Org. Chem. Jpn.* **2008**, *66*, 1211–1222; (g) Iyoda, M.; Nishinaga, T.; Takase, M. *Top. Heterocycl. Chem.* **2009**, *18*, 103–118.
6. (a) Iyoda, M. *Adv. Synth. Catal.* **2009**, *351*, 984–998; (b) Iyoda, M.; Hara, K.; Kuwatani, Y.; Nagase, S. *Org. Lett.* **2000**, *2*, 2217–2220.
7. (a) Iyoda, M.; Kuwatani, Y.; Ueno, N.; Oda, M. *J. Chem. Soc., Chem. Commun.* **1992**, 158–159; (b) Iyoda, M.; Hara, K.; Rao, C. R. V.; Kuwatani, Y.; Takimiya, K.; Morikami, A.; Aso, Y.; Otsubo, T. *Tetrahedron Lett.* **1999**, *40*, 5729–5730; (c) Iyoda, M.; Hara, K.; Ogura, E.; Takano, T.; Hasegawa, M.; Yoshida, M.; Kuwatani, Y.; Nishikawa, H.; Kikuchi, K.; Ikemoto, I.; Mori, T. *J. Solid State Chem.* **2002**, *168*, 597–607.
8. The reaction of tetrathiafulvalenyl bromides with magnesium could not afford the corresponding tetrathiafulvalenyl-magnesium bromides **5a–d**. Therefore, the two step procedure based on the first lithiation, followed by treatment with MgBr₂ was employed for the preparation of **5a–d**.
9. Compound **2b**: Red cryst., ¹H NMR (500 MHz, CDCl₃) δ 6.22 (s, 2H), 2.82 (m, 8H), 1.65–1.55 (m, 8H), 1.45 (m, 8H), 0.93 (t, J = 7.3 Hz, 12H), also see Refs. 2e,f.
10. Compound **2c**: Fine red needles, mp 116.5–118.5 °C. LDI-MS m/z 982 (M⁺); ¹H NMR (500 MHz, CDCl₃) δ 6.22 (s, 2H), 2.9–2.7 (m, 8H), 1.5–1.2 (m, 48H), 0.88 (t, J = 6.6 Hz, 12H). Anal. Calcd for C₄₄H₇₀S₁₂: C, 53.72; H, 7.17. Found: C, 53.50; H, 7.08.
11. Compound **2d**: Fine red fibrous material, mp 112–114 °C. LDI-MS m/z 1206 (M⁺); ¹H NMR (500 MHz, CDCl₃) δ 6.22 (s, 2H), 2.81 (m, 8H), 1.67–1.57 (m, 8H), 1.45–1.20 (m, 72H), 0.88 (t, J = 6.9 Hz, 12H). Anal. Calcd for C₆₀H₁₀₂S₁₂: C, 59.64; H, 8.12. Found: C, 59.39; H, 8.12.
12. Cyclic voltammetric analysis was carried out under the following conditions: 0.1 M Bu₄NClO₄ in dichloromethane, Ag/Ag⁺ reference electrode, Pt working electrode, and Pt counterelectrode, 100 mV s⁻¹; the oxidation potential of ferrocene, Fc/Fc⁺ = 0.29 V referred to Ag/Ag⁺.
13. The bulk conductivity at room temperature was measured in a compressed pellet by a two-probe technique.
14. (a) Sly, J.; Kasák, P.; Gomar-Nadal, E.; Rovira, C.; Górriz, L.; Thorarson, P.; Amabilino, D. B.; Rowan, A. E.; Nolte, R. J. M. *Chem. Commun.* **2005**, 1255–1257; (b) Akutagawa, T.; Kakiuchi, K.; Hasegawa, T.; Noro, S.; Nakamura, T.; Hasegawa, H.; Mashiko, S.; Becher, J. *Angew. Chem., Int. Ed.* **2005**, *44*, 7283–7287; (c) Kitamura, T.; Nakaso, S.; Mizoshita, N.; Tochigi, Y.; Shimomura, T.; Moriyama, M.; Ito, K.; Kato, T. *J. Am. Chem. Soc.* **2005**, *127*, 14769–14775; (d) Kitahara, T.; Shirakawa, M.; Kawano, S.; Beginn, U.; Fujita, N.; Shinkai, S. *J. Am. Chem. Soc.* **2005**, *127*, 14980–14981; (e) Wang, C.; Zhang, D.; Zhu, D. *J. Am. Chem. Soc.* **2005**, *127*, 16372–16373.
15. Reported intermolecular distances of stacked tetrakis(alkylthio)-tetrathiafulvalenes (TTC_n-TTFs) are 4.7 Å for TTC₈-TTF, 4.5 Å for TTC₁₄-TTF, and 4.4 Å for TTC₁₈-TTF: Ukai, S.; Igarashi, S.; Nakajima, M.; Marumoto, K.; Ito, H.; Kuroda, S.; Nishimura, K.; Emoto, Y.; Saito, G. *Colloid Surf. A, Physicochem. Eng. Aspects* **2006**, *284–285*, 589–593.
16. Recently, a doped TTF-diamide was found to exhibit metallic spectroscopy curves when probed by current-sensing AFM: Puigmartí-Luis, J.; Minoia, A.; del Pino, Á. P.; Ujaque, G.; Rovira, C.; Lledós, A.; Lazzaroni, R.; Amabilino, D. B. *Chem. Eur. J.* **2006**, *12*, 9161–9175.
17. The current-sensing AFM of the **2d** fiber was performed on an HOPG surface using Shimadzu SPM-9600. I–V plots obtained for the needles with a grounded conducting Pt–Ir-coated silicon tip (CONTPt, NANO WORLD) show slightly p-type semiconducting behavior.